Inorganic Chemistry

Article

pubs.acs.org/IC

Reactivity and Speciation of Anti-Diabetic Vanadium Complexes in Whole Blood and Its Components: The Important Role of Red Blood Cells

Aviva Levina,[†] Andrew I. McLeod,[†] Sylvia J. Gasparini,[†] Annie Nguyen,[†] W. G. Manori De Silva,[†] Jade B. Aitken,[†,‡] Hugh H. Harris,[†] Chris Glover,[‡] Bernt Johannessen,[‡] and Peter A. Lay*[,†]

[†]School of Chemistry, The University of Sydney, Sydney NSW 2006, Australia

[‡]Australian Synchrotron, 800 Blackburn Rd., Clayton VIC 3168, Australia

Supporting Information

ABSTRACT: Reactions with blood components are crucial for controlling the antidiabetic, anticancer, and other biological activities of V(V) and V(IV) complexes. Despite extensive studies of V(V) and V(IV) reactions with the major blood proteins (albumin and transferrin), reactions with whole blood and red blood cells (RBC) have been studied rarely. A detailed speciation study of $Na_3[V^VO_4]$ (**A**), $K_4[V^{IV}_2O_2(citr)_2]\cdot 6H_2O$ (**B**; citr = citrato(4−)); $[V^{IV}O(ma)_2]$ (**C**; ma = maltolato(−)), and $(NH_4)[V^V(O)_2(dipic)]$ (**D**; dipic = pyridine-2,6-dicarboxylato(2−)) in whole rat blood, freshly isolated rat plasma, and commercial bovine serum using X-ray absorption near-edge structure (XANES) spectroscopy is reported. The latter two compounds are potential oral antidiabetic drugs, and the former two are likely to represent their typical decomposition products in gastrointestinal media. XANES spectral speciation was performed by principal component analysis and multiple linear regression techniques, and the distribution of V between RBC and plasma fractions was measured by electrothermal atomic absorption spectroscopy. Reactions of **A**, **C**, or **D** with whole blood (1.0 mM V, 1−6 h at 310 K) led to accumulation of ∼50% of total V in the RBC fraction (∼10% in the case of **B**), which indicated that RBC act as V carriers to peripheral organs. The spectra of V products in RBC were independent of the initial V complex, and were best fitted by a combination of V(IV)−carbohydrate (2-hydroxyacid moieties) and/or citrate (65−85%) and V(V)−protein (15−35%) models. The presence of RBC created a more reducing environment in the plasma fraction of whole blood compared with those in isolated plasma or serum, as shown by the differences in distribution of V(IV) and V(V) species in the reaction products of **A**−**D** in these media. At physiologically relevant V concentrations (<50 μM), this role of RBC may promote the formation of V(III)-transferrin as a major V carrier in the blood plasma. The results reported herein have broad implications for the roles of RBC in the transport and speciation of metal pro-drugs that have broad applications across medicine.

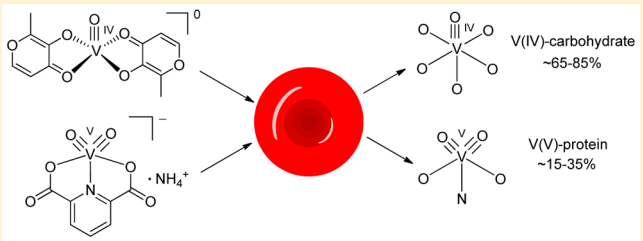

INTRODUCTION

Diverse biological roles of vanadium complexes, including antidiabetic, cardioprotective, radioprotective, osteogenic, as well as anticancer and antiparasitic activities, have been extensively studied over the last three decades.[1−9] Generally, V(V) and V(IV) complexes with organic ligands are pro-drugs that react with biological media with the release of active components, such as vanadates or peroxido-vanadates, which then act as potent inhibitors of protein tyrosine phosphatases and alter cell signaling.[2−4,6,10] Considerable attention has been paid to the reactions of biologically active V(V) and V(IV) complexes with major blood serum proteins, such as albumin, immunoglobulins, and transferrin,[11−14] but relatively little research has been conducted on the reactions of V complexes with whole blood,[15,16] or with red blood cells (RBC).[17−22] The role of RBC in the pharmacokinetics of V-based drugs was previously assumed to be neglible,[12a] but recent data have pointed to their potential importance as carriers of V to peripheral organs.[22,23] Further advances in the understanding of the roles of RBC and other biological components in V metabolism have been hampered by several analytical limitations. First, the two spectroscopic techniques that are most commonly used for the speciation of V in biological systems require relatively large (millimolar) V concentrations, and are sensitive to only one of the biologically relevant oxidation states of V (electron paramagnetic resonance (EPR) spectroscopy for V(IV) and ^{51}V NMR spectroscopy for V(V)).[4,12a] Reduction of V(V) or V(IV) to V(III) in tunicates (V-accumulating sea organisms) is well-known, although its physiological role has not been elucidated as yet.[24] The possibility that V(III) is accessible in mammalian organisms has also been suggested,[12c] but no reliable method for its detection in the presence of V(IV) and V(V) existed until our recent studies.[25] Second, methods based on the separation of V-bound biomolecules by chromatographic or electrophoretic techniques

Received: March 24, 2015
Published: July 31, 2015

DOI: 10.1021/acs.inorgchem.5b00665
Inorg. Chem. 2015, 54, 7753−7766

often lead to unreliable results, due to the generally low stability of V-biomolecule adducts under the conditions used for their analysis.[26,27]

Over the past decade, X-ray absorption near edge structure (XANES) spectroscopy has become a method of choice for speciation studies of metal ions in complex matrices, including biological fluids, cells, and tissues.[28] Our group has previously applied this technique to reactivity studies of toxic (Cr(VI)) and medicinal (Cr(III), Mo(VI), Ru(III)) metal ions in biological media.[29] Recently, we developed a general method for the determination of oxidation states and coordination numbers of V ions in biological and environmental samples, using a library of XANES spectra of biologically relevant V(V), V(IV), and V(III) complexes.[25] This method has been subsequently used to study the reactivities of typical oral antidiabetic V(V) and V(IV) drugs in gastrointestinal environments,[30a] in potential pharmaceutical formulations,[30b] and in cultured mammalian cells and cell culture media.[30c] Here, we present the first XANES spectroscopic study of the reactivities of biologically relevant V(V) and V(IV) complexes with whole rat blood and its components. The compounds chosen for this study (**A**–**D** in Chart 1) include potential oral antidiabetic drugs (**C** and **D**)[31,32] and likely models of their decomposition products in gastrointestinal media (**A** and **B**).[30a] Note that V-oxido binding in V(IV) complexes is represented with triple, rather than double, bonds (contrary to a common convention), which arise from a combination of one σ and two π bonds, while the bond order in dioxido V(V) complexes (Chart 1) is close to 2.5.[30c,33,34]

Chart 1. Structures of V Complexes Used for the V Reactions with Blood or Its Components (A–D) and Additional Model Complexes (E–I)[25] Used in the Data Analysis[a]

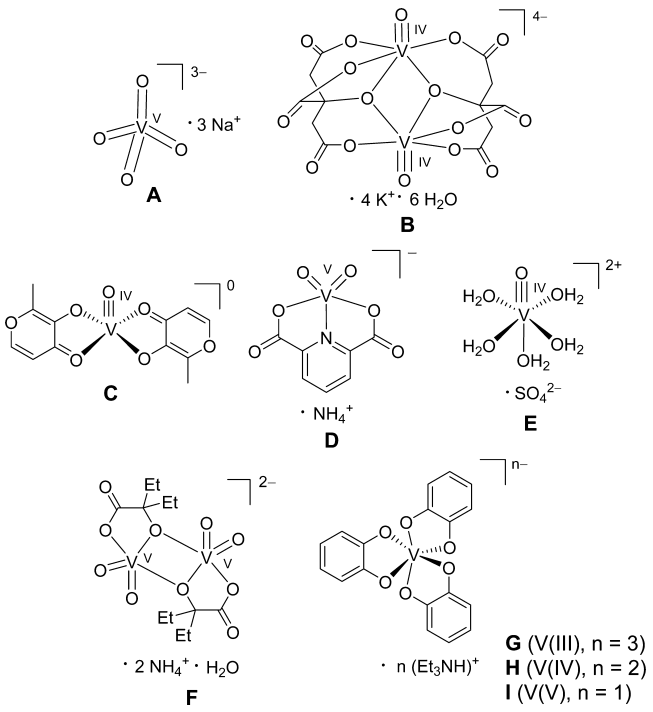

[a]The V-oxido binding in V(IV) complexes (**B**, **C**, and **E**) is represented by triple, rather than double, bonds (a combination of one σ and two π bonds), while the bond order in V(V) dioxido complexes (represented as double bonds in **D** and **F**) is close to 2.5[30c,33,34].

Two recent articles[22] on the interactions of antidiabetic V(IV) complexes with RBC or with isolated hemoglobin (Hb, studied by EPR spectroscopy) have appeared. The key differences between our research and these published data[22] are as follows. First, XANES spectroscopy used in our work provided simultaneous detection and quantitation of V(V), V(IV), and V(III) oxidation states,[25,28,30] rather than of V(IV) only, as in the previous studies by EPR spectroscopy.[11−13,22] Second, unlike for most previous studies that used RBC suspensions in aqueous buffers,[18−22] the present research used whole blood (including RBC and plasma fractions), which provided a more biologically relevant situation.[15,16] Finally, the current study included the interactions of representative V products of gastrointestinal digestion (**A** and **B** in Chart 1)[30] with blood components. By contrast, previous speciation studies[11−13,22] assumed that orally administered V antidiabetics reach the blood unchanged, which was clearly not the case,[30a] at least in part.

EXPERIMENTAL SECTION

Materials and Sample Preparation. The V(V) and V(IV) complexes used to study the reactions with blood and its components (**A**–**D** in Chart 1) were either purchased from Aldrich (**A**; >99%), or synthesized by modified literature procedures (**B**–**D**)[35−38] and characterized by elemental analyses, infrared spectroscopy, and electrospray mass spectrometry, as described previously.[25] Newborn calf serum (heat-inactivated and filtered) was purchased from Invitrogen. Other reagents of analytical or higher purity grade were purchased from Sigma-Aldrich or Merck and used without further purification. Water was purified by the Milli-Q technique. Blood samples were obtained by cardiac puncture from healthy male Sprague–Dawley rats that were handled in accordance with the policy of the University of Sydney (Animal Ethics Approval L07/1–2004/3/3846). Whole blood was collected into heparin-coated Vacutainer tubes (Becton Dickinson), kept on ice prior to experimentation, and used within 2 h of collection. A portion of whole blood was centrifuged (5000 g for 10 min at 277 K), and the supernatant plasma was removed for the reactivity studies with **A**–**D**.

The conditions used for sample preparations for XANES measurements are listed in Table 1. Stock solutions of V(V) and V(IV) complexes (50 mM for **A**, **B**, and **D** or 10 mM for **C**) in physiological saline (0.15 M NaCl in H_2O) were prepared within 1 h before the experiments (**C** was dissolved by sonication for 10 min at 295 K under Ar atmosphere). The stock solutions were then added to whole blood, isolated plasma, or serum (0.30 mL of biological fluids per sample) to a final V concentration of 1.0 mM, and the reactions were performed at 310 K under ambient air conditions for 1 or 6 h. After the reactions, the plasma and serum samples were immediately frozen at 193 K and freeze-dried (217 K, 0.5 mbar for 20 h). Whole blood samples were separated into RBC and plasma fractions by centrifugation (5000 g for 10 min at 277 K), then both fractions were frozen and freeze-dried separately. The buffy coat was removed from the top of the RBC pellets after freeze-drying, but these fractions were too small to be analyzed separately. The freeze-dried samples were kept desiccated at 277 K for 1–2 weeks prior to the analyses. In addition, the reactions of **A** with purified bovine proteins, including serum albumin (BSA; Sigma A3059), apo-transferrin (Tf; Sigma T4382) and met-hemoglobin (Hb; Sigma H2500) were performed in HEPES-buffered aqueous solutions, where HEPES = 4-(2-hydroxyethyl)piperazine-1-ethanesulfonic acid (details of the reaction conditions are listed in Table 1), and the samples were freeze-dried and stored as described above. The buffers used for the preparation of **A**-BSA and **A**-Tf samples (Table 1) also contained carbonate, which is a synergistic ion required for the binding of V(III) or V(IV), but not V(V), to the specific Fe(III) binding sites of Tf.[12a]

DOI: 10.1021/acs.inorgchem.5b00665
Inorg. Chem. 2015, 54, 7753–7766

Table 1. Samples Used for XANES Spectroscopic Speciation

label[a]	reaction medium[b]
A1_1h; **A1**_6h	whole blood, then RBC separated and measured
A2_1h; **A2**_6h; **A2**_6h*	whole blood, then plasma separated and measured
A3_1h; **A3**_6h; **A3**_6h*	freshly isolated plasma
A4_1h; **A4**_6h; **A4**_6h*	commercial bovine serum
B1_1h; **B1**_6h	whole blood, then RBC separated and measured
B2_1h; **B2**_6h	whole blood, then plasma separated and measured
B3_1h; **B3**_6h	freshly isolated plasma
B4_1h; **B4**_6h	commercial bovine serum
C1_1h; **C1**_6h; **C1**_6h*	whole blood, then RBC separated and measured
C2_1h; **C2**_6h; **C2**_6h*	whole blood, then plasma separated and measured
C3_1h; **C3**_6h; **C3**_6h*	freshly isolated plasma
C4_1h; **C4**_6h; **C4**_6h*	commercial bovine serum
D1_1h; **D1**_6h	whole blood, then RBC separated and measured
D2_1h; **D2**_6h	whole blood, then plasma separated and measured
D3_1h; **D3**_6h	freshly isolated plasma
D4_1h; **D4**_6h	commercial bovine serum
A-BSA	0.50 mM **A** + 0.50 mM BSA in 100 mM HEPES, 25 mM $NaHCO_3$, pH = 7.40 for 4 h at 310 K
A-Tf	0.50 mM **A** + 0.50 mM Tf in 100 mM HEPES, 25 mM $NaHCO_3$, pH = 7.40 for 4 h at 310 K
A-Hb*	1.0 mM **A** + 0.078 mM Hb in 20 mM HEPES, 140 mM NaCl, pH = 7.40 for 24 h at 310 K

[a]Complex designations (**A**, **B**, **C**, or **D**) correspond to those in Chart 1, the bold numbers designate the reaction media (**1** for the RBC fraction, **2** for the plasma fraction of whole blood, **3** for the isolated rat plasma and **4** for commercial bovine serum), and 1h or 6h designate the reaction times, 1 or 6 h, respectively, at 310 K. The samples were freeze-dried after the reactions, and XANES data were collected at 295 K (Experimental for details). For the samples designated with asterisks, the XANES data were collected at ANBF, and the rest of the data were collected at AS (separate aliquots of the same sample were used to collect data at both AS and ANBF). [b]Initial V concentrations were 1.0 mM, unless specified otherwise. Abbreviations: RBC = red blood cells, BSA = bovine serum albumin, Tf = bovine apoTf, Hb = bovine met-hemoglobin, HEPES = 4-(2-hydroxyethyl)piperazine-1-ethanesulfonic acid.

For the kinetics studies of V distribution between the plasma and cell fractions, blood samples (30 μL per sample) were incubated with **A**–**D** ([V] = 1.0 mM) for 0–6 h at 310 K, then cooled on ice and centrifuged (10 000 g for 5 min at 277 K). For zero time points, compounds **A**–**D** were added to the blood samples on ice, and the samples were immediately centrifuged at 277 K. Separated blood cell and plasma fractions were digested with ultrapure HNO_3 (Merck; 69% w/v in H_2O; 0.20 mL per sample) by sonication (1 h at 50 W and 295 K) and brought to 1.0 mL volume with ultrapure HCl solution (0.10 M, prepared from 37% w/v stock, Merck). The V content in the resultant solutions was determined by electrothermal atomic absorption spectroscopy with an Agilent 240Z spectrometer (Agilent Technologies; equipped with Zeeman background correction), using standard V(IV) solutions in 0.10 M HCl (Aldrich) for calibration. In a separate kinetic experiment, aliquots of plasma fraction only (10 μL) were taken from the samples after centrifugation, and the V content was determined as described above.

XANES Spectroscopy and Data Processing. Vanadium K-edge spectra of all of the samples listed in Table 1 (except for V-Hb) were recorded at the X-ray Absorption Spectroscopy Beamline, Australian Synchrotron (AS, Melbourne, Australia).[39] The electron beam energy was 3.0 GeV, and the maximal current was 200 mA. The beamline had a double-crystal Si[111] monochromator, an upstream collimating mirror (Si-coated), and a downstream sagittally focusing mirror (Rh-coated). Additionally, a third mirror (SiO_2-coated) downstream from the focusing mirror provided harmonic rejection so that harmonics made a negligible contribution to the X-ray absorption spectroscopy (XAS). Neat freeze-dried samples were pressed into 0.5 mm thick pellets that were supported within a polycarbonate spacer between two 63.5 μm Kapton tape windows (window size, 2 × 10 mm). The samples were placed in a He-filled box at ~295 K, and the XANES data were collected in fluorescence detection mode, using a Ge planar detector (Eurisys; 100-element). Low-temperature XAS measurements were not used, since they led to a significant reduction in the signal-to-noise ratio, due to the strong absorption of photons over the 5–6 keV energy range by the cryostat windows and air between the cryostat and detector. For all of the samples, only XANES regions were recorded (5250–5700 eV range; step sizes, 10 eV below 5450 eV, 0.25 eV at 5450–5525, and 2 eV above 5525 eV). The dwell time per point was 2.0 s for most samples, or 0.50 s for rapid scans for X-ray sensitive samples. The energy scale was calibrated using a V foil as an internal standard (calibration energy, 5465.0 eV, corresponding to the first peak of the first derivative of V(0) edge).[40] In addition, XANES spectra of selected samples (Table 1; different aliquots of the same preparations) were recorded at ~295 K in the fluorescence detection mode at the Australian National Beamline Facility (ANBF, beamline 20B, Photon Factory, KEK, Tsukuba, Japan), while the spectrum of **A**-Hb (Table 1) was recorded at the ANBF only.

The beam energy at ANBF was 2.5 GeV, and the maximal beam current was 400 mA. The beamline was equipped with a channel-cut Si[111] monochromator and a 36-element planar Ge detector (Eurisys). The monochromator was detuned by 50% to reduce harmonic contributions. Other experimental conditions at ANBF were identical to those at the AS. No significant photodamage of the samples occurred at ANBF (as shown by comparison of XANES data from sequential scans), while the relative intensities of the pre-edge peaks decreased by ≥5% by the second scans of the samples recorded at AS, which indicated a significant level of photodamage.[41] The extent of photodamage was higher at the AS compared with the ANBF because of the higher photon flux, but this also provided higher signal-to-noise ratios.[41] The XANES of model complexes were recorded at AS (solid mixtures with boron nitride, 295 K) for **A**–**F** (Chart 1), or resplined from published data (for **G**–**I** in Chart 1),[42] as described previously.[25]

Calibration, averaging, and splining of XANES data were performed using the Average and Spline programs within XFit software package.[43] The spectra were normalized according to the method of Penner-Hahn and co-workers,[44] to match the tabulated X-ray cross-section data[45] for V (in a similar manner to the earlier work on Cr(III) XANES spectra).[29b] This normalization technique led to consistent XANES spectra for all of the samples, regardless of the beamline used and the signal-to-noise ratio. Principal component analyses of the normalized XANES data were performed using Unscrambler software.[46] Multiple linear regression analyses of XANES data were performed using Origin software[47] with previously described criteria for a successful fit.[29a] Initially, the full set of spectra for model complexes[25] was used for multiple linear regression analyses, but most of the spectral models were rejected computationally during the fitting algorithm due to negative regression coefficients.[29a]

RESULTS

Distribution of Vanadium Complexes between Cell and Plasma Fractions. Figure 1a shows time-dependent V distributions between the plasma and cell (RBC and buffy coat) fractions of whole rat blood after incubations with compounds **A**–**D** (1.0 mM V) for 0–6 h at 310 K as determined by atomic absorption spectroscopy (AAS). Longer incubation times were not used, since they led to visible RBC lysis (red coloration of the plasma fraction). The lowest V content in the cell fractions at zero time points (273–277 K; ~30% of total V, Figure 1a)

DOI: 10.1021/acs.inorgchem.5b00665
Inorg. Chem. 2015, 54, 7753–7766

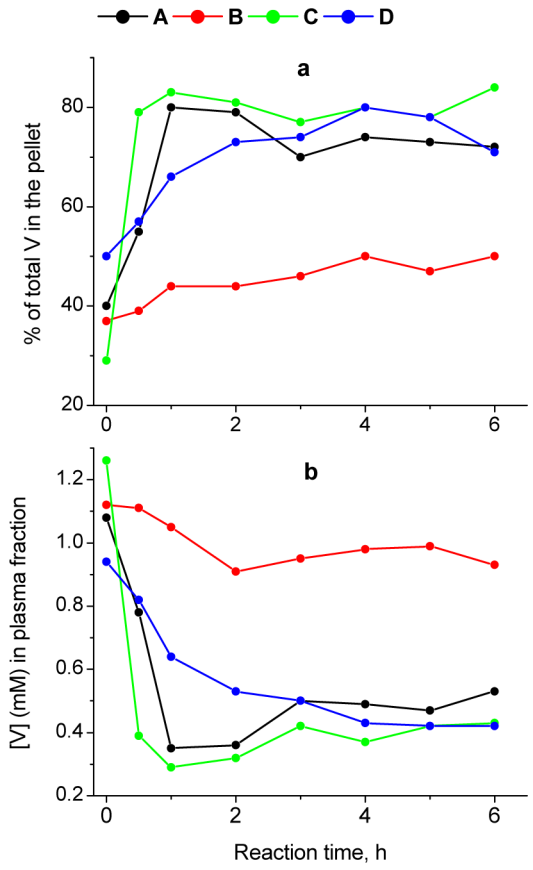

Figure 1. AAS determinations of time-dependent V distribution between the cell pellet (RBC and buffy coat) and plasma fractions of whole blood (the % includes that contained within the plasma that was retained in the pellet and the % at time 0 h needs to be subtracted from the total % to obtain that contained within the RBC fraction) (a); and changes in plasma V concentration (b) during the treatment of whole blood with **A**-**D** (Chart 1; 1.0 mM V) for 1−6 h at 310 K. The data in (a) and (b) were obtained in separate kinetic experiments (Experimental section).

corresponded to the amount of V in residual plasma in the pellets (which were not washed to avoid V leaching from the cells).[18] Incubation of whole blood with either **A** or **C** at 310 K led to rapid increases of relative V content in the pellets (to ∼80% within 1 h; black and green lines in Figure 1a), followed by less prominent changes within the next 5 h. In the case of **D**, rapid RBC uptake of V occurred even at 273−277 K (relative V content in the pellet was ∼50% at zero time point), followed by a slower increase to ∼80% V content in the pellet within the next 6 h at 310 K (blue line in Figure 1a). The RBC uptake of V from **B** was significantly lower than that for the other three compounds (red line in Figure 1a). These results were confirmed in a separate experiment where the V content was determined in the plasma fraction only (Figure 1b). Notably, both experiments showed small but significant increases of V concentration in the plasma fraction for **A** and **C**, which followed the initial rapid decreases (black and green lines in Figures 1a,b). These results indicated that the uptake of V(V) or V(IV) species by intact RBC was a reversible process, although the forward process was faster than the reverse one, in agreement with published data.[18] Equilibrium V concentrations in the plasma fraction were ∼45−50% of total V for the treatments with **A**, **C**, or **D** and ∼90% in the case of **B** (Figure 1a,b). The remaining V was mostly taken up by RBCs, since mammalian blood typically contains one white blood cell and 40 platelets per 600−700 RBCs.[48] Note that the reactions of **A**−**D** with the plasma components occurred at comparable rates to those from the V uptake by the cells as shown by the XANES below. The data contained in Figure 1a,b justified the choice of time points for the XANES spectroscopic studies of RBC and plasma fractions of V-treated blood (Table 1): 1 h as the end of rapid RBC uptake phase for **A** and **C** and 6 h as the point when an equilibrium was reached for all four compounds, but no significant cell lysis had yet occurred.

Vanadium Speciation in the Reaction Products with Blood and its Components. Conditions used for XANES sample preparation (Table 1) included treatments of whole blood with compounds **A**−**D** (V concentration, 1.0 mM) for 1 or 6 at 310 K, followed by the separation of RBC and plasma fractions, and data collection for both fractions (samples **A1**−**D1** and **A2**−**D2**, respectively, in Table 1). Analogous treatments were performed in freshly isolated rat plasma (samples **A3**−**D3**) and in commercial (heat-inactivated and filtered) bovine serum (samples **A4**−**D4**). The XANES data were collected both at the AS (for all of the blood samples listed in Table 1) and at the ANBF (for selected samples; Table 1 and Experimental for details).

Figure 2 shows typical XANES of the reaction products compared with those of the model complexes.[25] As was observed previously for the reactions of metal-based drugs with biological media,[29,30] reactions of **A**−**D** with whole blood or with isolated plasma or serum for 1 h at 310 K resulted in convergence of very different spectra of the initial species (Figure 2a) into similar spectra of the bio-transformation products (Figure 2b−d). The positions and intensities of pre-edge peaks (due to the symmetry-forbidden 1s → 3d transition)[49,50] and the edge energies (typically determined at half-edge jump)[25,51] are the key XANES parameters that reflect the oxidation states and coordination numbers of the V species in a wide variety of inorganic and organic matrices.[25,51,52]

A comparison of these parameters for the spectra of V biotransformation products (Table 1; AS data only, excluding the reaction products with purified proteins) with those of model V(V) and V(IV) oxido complexes[25] is shown in Figure 3. Both the three-dimensional plot (Figure 3a)[25] and its projections into separate axes (Figure 3b-d) were consistent with the predominance of six-coordinate V(IV) and five-coordinate V(V) oxido complexes in the reaction products of **A**−**D** with blood components (Table 1). In particular, pre-edge peak positions in the XANES of the reaction products were consistent with those for six-coordinate V(IV) and five- or four-coordinate V(V) complexes, but not for five-coordinate V(IV) or six-coordinate V(V) complexes (Figure 3c). Octahedral nonoxido V(V), V(IV), or V(III) complexes can be ruled out as major components of the reaction products because of the low pre-edge peak intensities in their XANES spectra (<5% of the edge jump; Figure 3a),[25,42] but their presence as minor components cannot be excluded. A comparison of XANES parameters for the groups of samples (that were dependent on the reaction medium, Figure 3e) showed that the XANES of the reaction products with isolated plasma or serum tended to have higher edge energies and pre-edge heights and, hence, higher V oxidation states, compared with those in whole blood, but all the groups were significantly mixed (Figure 3e).

Results of principal component analyses (PCA)[29a,53] of the XANES data (Table 1; AS data only, excluding the reaction products with purified proteins) are shown in Figure 4. A clear

DOI: 10.1021/acs.inorgchem.5b00665
Inorg. Chem. 2015, 54, 7753−7766

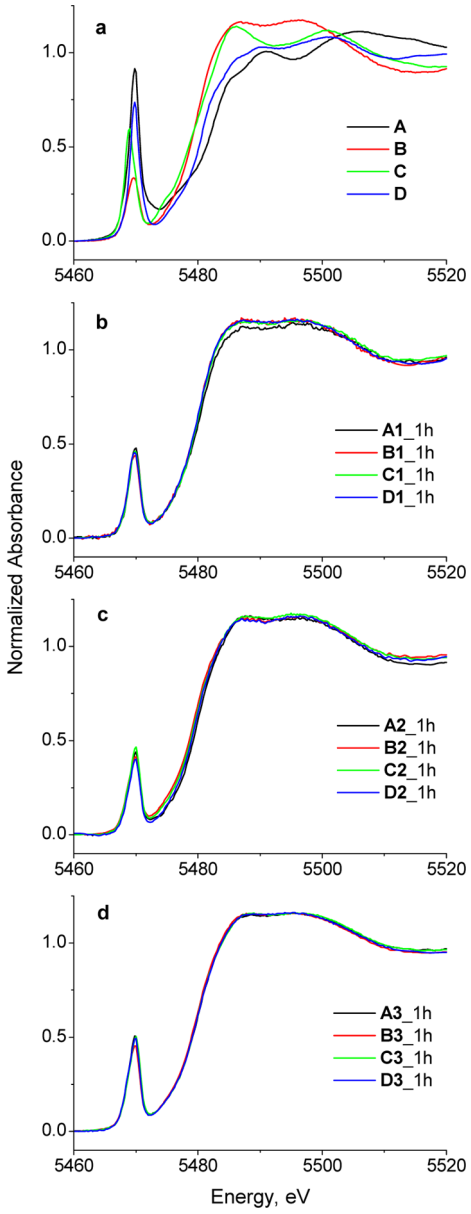

Figure 2. (a) XANES spectra of the initial V(V) and V(IV) complexes **A**–**D** (Chart 1; from previously reported data).[25] (b–d) Typical XANES spectra of the reaction products with blood and its components (designations correspond to those in Table 1). All of the spectra were measured at the AS at 295 K (see Experimental Section).

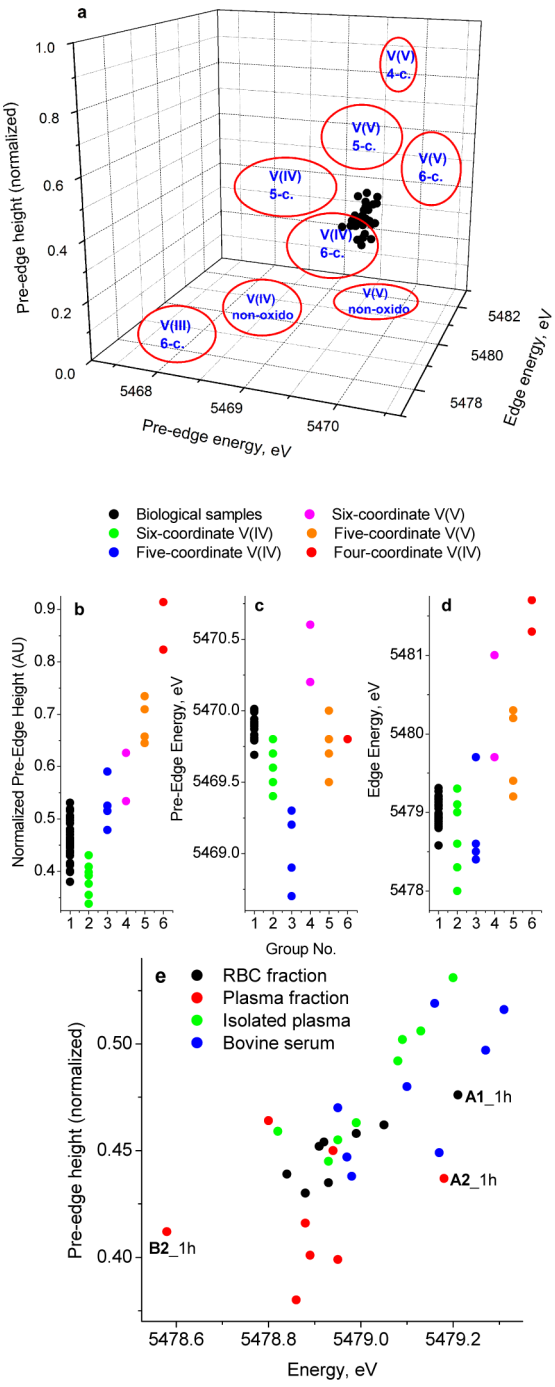

Figure 3. Comparison of key parameters of XANES spectra[25,51,52] for the reaction products of **A**–**D** with blood and its components (Table 1, AS data only, excluding the reaction products with purified proteins) and for model V(V), V(IV) and V(III) complexes (based on previously published data).[25] **a:** Three-dimensional plot[25] of XANES parameters for biological samples (represented with black dots) and groups of model complexes (red circles, grouped by V oxidation states and coordination numbers) for which the values of edge energies were determined at the half-edge jump.[25,51] **b-d:** Projections of the data shown in (**a**) to separate axes. **e:** Comparison of edge energies and pre-edge heights for the biological samples grouped by the reaction medium (Table 1).

separation between XANES of both fractions of whole blood, on the one hand, and of the isolated plasma or serum samples, on the other, was achieved based on the two first principal components (PC1 and PC2 in Figure 4), which constituted 58.5% and 17.3% of total variance, respectively. In addition, XANES of the RBC and plasma fractions of whole blood (black and red dots in Figure 4a) were separated based on the third principal component (PC3, 8.5% of total variance), but no such separation was evident for the isolated plasma and serum samples (green and blue dots in Figure 4a). As shown in Figure 4b, significant differences between the groups of samples were observed in the pre-edge, edge, and postedge areas. No separation of the XANES data by PCA could be achieved based on either the initial V compound (**A**–**D**) or the reaction time (1 or 6 h), as shown in Figure S1 (Supporting Information).

DOI: 10.1021/acs.inorgchem.5b00665
Inorg. Chem. 2015, 54, 7753–7766

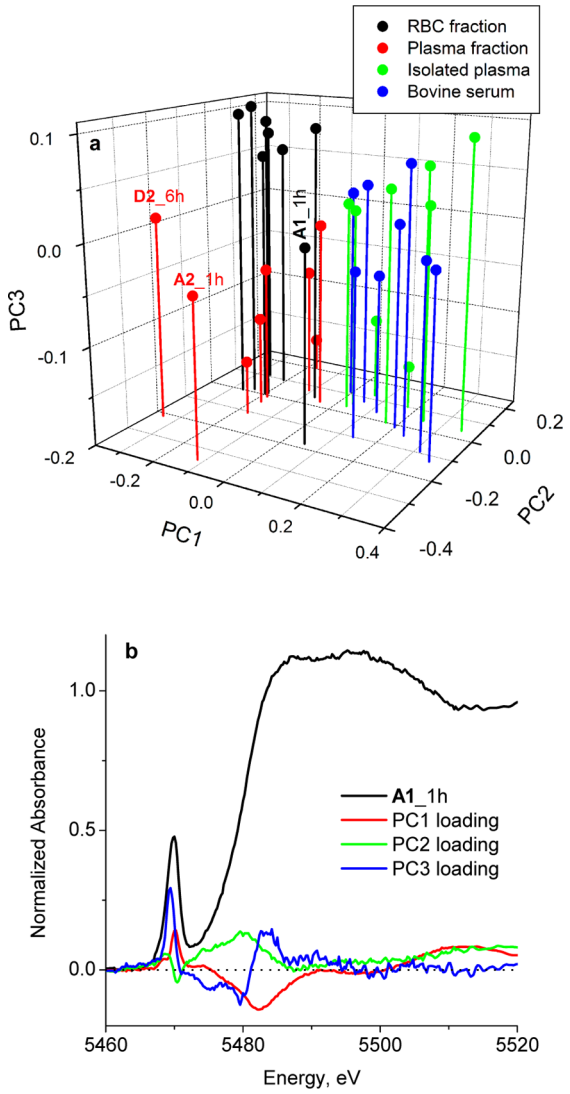

Figure 4. a: Scores plot of the first three principal components (representing 58.5%, 17.3% and 8.5% of total variation, respectively) for the set of XANES data listed in Table 1 (AS data only, excluding the reaction products with purified proteins). **b:** Comparison of a typical XANES spectrum for a V reaction product (**A1**_1h in Table 1) and the first three loading plots for all the samples included in (**a**). The XANES spectra were normalized as described in the Experimental section and were used for PCA (performed with Unscrambler software)[46] without further processing. Additional PCA results are shown in Figure S1 (Supporting Information).

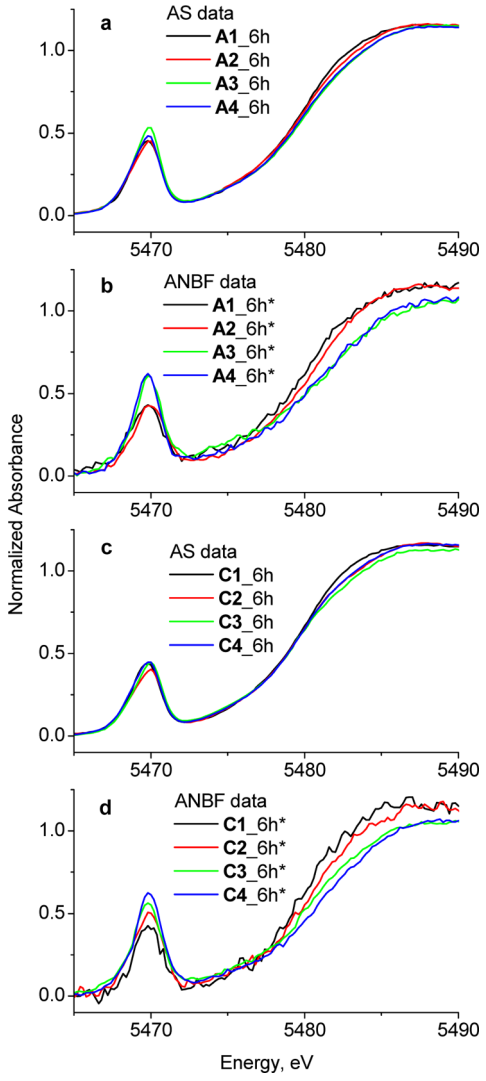

Figure 5. Pre-edge and edge areas of XANES spectra (neat freeze-dried samples, 295 K) for selected reaction products of whole blood or its components with compounds **A** or **C** (1.0 mM V) for 6 h at 310 K. Designations of the samples correspond to those in Table 1. Separate aliquots of the same samples were used for data collection at either AS (**a**,**c**) or ANBF (**b**,**d**). See the Experimental Section for the parameters used for the measurements at each of the beamlines.

Figure 5 highlights changes in the pre-edge and edge areas of XANES spectra (5460−5490 eV) as a function the beamline used for data collection. These spectral regions contain essential information about the oxidation states and coordination numbers of V species.[25,51,52] In agreement with the data in Figure 3e, the spectra shown in Figure 5a,c (data collected at AS) pointed to small but significant increases in average V oxidation states for the V reaction products with isolated plasma or serum (samples **A3**−**D3** and **A4**−**D4** in Table 1) compared to those in the fractions of whole blood (**A1**−**D1** and **A2**−**D2** in Table 1).

The differences between the samples derived from whole blood treatments and those obtained from isolated plasma or serum were much more evident for the data collected at ANBF (Figure 5b,d). Because of the higher photon flux at AS compared with ANBF, the former data were more likely to be affected by photodamage (Experimental Section), but they also had higher signal-to-noise ratio (Figure 5).[41] For the RBC samples (**A1**_6h and **C1**_6h), the XANES data collected at either AS or ANBF agreed within experimental noise level (Figure 5 and Figure S2 in Supporting Information). A small but significant amount of photoreduction at AS was evident (by comparison with the ANBF data) for the samples of blood plasma fractions (**A2**_6h and **C2**_6h), but this was considerable for the samples of isolated plasma or serum (**A3**_6h, **C3**_6h, **A4**_6h and **C4**_6h; Figures 5 and S2), which is addressed below.

Multiple Linear Regression Analyses of XANES Data. The analyses[29a,54] for the samples listed in Table 1 (both AS and ANBF data, excluding the data for **A**-BSA, **A**-Tf, and **A**-Hb) were performed with the use of the previously developed XANES library of biologically relevant V(V), V(IV), and V(III) complexes.[25] The best fits (Figure 6) included contributions

DOI: 10.1021/acs.inorgchem.5b00665
Inorg. Chem. 2015, 54, 7753−7766

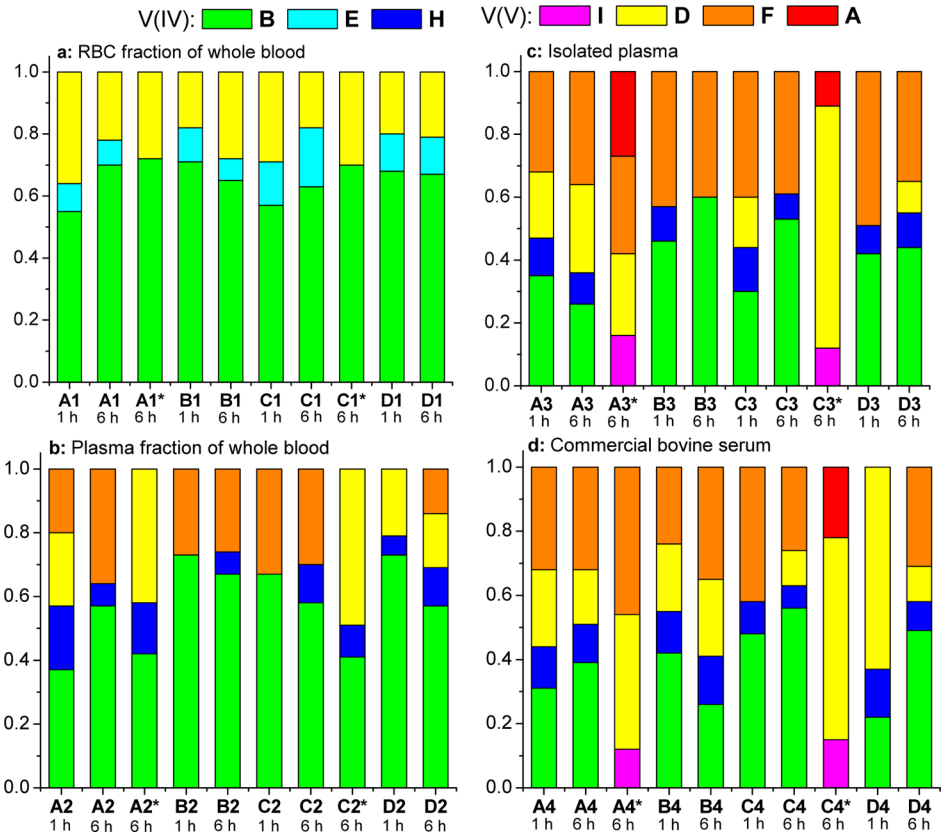

Figure 6. Summary of multiple linear regression analysis results of XANES data (Tables S1 and S2 and Figures S3 and S4 in Supporting Information provide detailed fit results and overlays of experimental and fitted spectra) for the samples listed in Table 1 (excluding the samples **A**-BSA, **A**-Tf, and **A**-Hb). The data designated as **A1***–**A4*** and **C1***–**C4*** were collected at ANBF (Figure 5b,d), and all of the other data were collected at AS. The Experimental Section provides the parameters used for measurements at both beamlines.

from the XANES of models **A**, **B**, **D**, **E**, **F**, **H**, and **I** (Chart 1), among which were six-coordinate V(IV) monooxido complexes (**B** and **E**),[35,55] four-coordinate V(V) tetraoxido (**A**), and five-coordinate V(V) dioxido complexes (**D** and **F**),[36,56] as well as nonoxido V(IV) and V(V) complexes (**H** and **I**),[42] all with exclusively or predominantly O-donor ligands. Detailed results of multiple linear regression analyses are given in Supporting Information Tables S1 and S2, and overlays of experimental and fitted spectra are shown in Figures S3 (AS data) and S4 (ANBF data) in Supporting Information. As shown in Figures S3 and S4, satisfactory fits of the pre-edge and edge XANES areas (5460–5490 eV) were achieved for all the samples, which was supported by comparison of numerical values of the fit residues and the corresponding values for the differences between different samples (Table S2). Notably, the lowest fit residues were consistently obtained for the XANES of RBC fractions compared with those from other sample types (Table S2 and Figures S3 and S4). Significant deviations between experimental and fitted spectra in the postedge areas (5490–5520 eV) were observed for most of the samples that were affected by photodamage (AS data for **A3**–**D3** and **A4**–**D4**; Figure S3). These deviations were likely to be due to the formation of V photoreduction products that were not adequately covered by the current model library. However, good fits of the pre-edge and edge XANES (Figures S3 and S4) were expected to provide reliable information on the average oxidation states and coordination environments of V species in these samples.[25] Multiple linear regression analyses of XANES data for all the RBC fractions (**A1**–**D1** in Table 1 and Figure 6a) resulted in similar fits, which included predominantly XANES from models **B** (V(IV), ~70% mol) and **D** (V(V), 15–25% mol), as well as (in most cases) small but significant proportions of **E** (V(IV), 7–12% mol). These results were consistent with the tight clustering of the RBC data in the PCA scores plots (black dots in Figure 4a), as well as with the analysis of XANES parameters in Figure 3. The only RBC sample that stood out in PCA (**A1**_1h in Figures 3e and 4a; treatment of whole blood with **A** for 1 h) was distinguished by a higher proportion of V(V) species (36% mol of model **D**; Figure 6a and Table S1), which is likely to be due to the incomplete V(V) reduction in RBC at this early stages of the reaction. Consistent XANES fits for RBC samples were obtained for data collected at either the AS or ANBF, although the presence of XANES from model **E** was not detected in fits to the latter data (designated as **A1b*** and **C1b*** in Figure 6a) due to the higher noise levels (Figures S3 and S4).

Several types of changes were observed in the XANES fits for plasma fractions separated from V-treated blood compared with the corresponding RBC samples (Figure 6a,b). For most of the XAS data collected at the AS (samples **A2a**, **A2b**, **B2a**, **B2b**, **C2a**, **C2b**, and **D2b** in Table 1 and Figure 6b), the best fits had full or partial replacement of XAS from model **D** with that from another five-coordinate V(V) model, **F** (Chart 1). On the other hand, best fits to the ANBF data (designated as **A2b*** and **C2b*** in Figure 6b), which were less affected by photodamage,[41] had an increase in the proportion of the XAS from model **D** in plasma fractions compared with those from the corresponding RBC fractions (**A1b*** and **C1b*** in Figure 6a).

DOI: 10.1021/acs.inorgchem.5b00665
Inorg. Chem. 2015, 54, 7753–7766

These results show that multiple linear regression analyses of XANES data are unlikely to distinguish with certainty between coordination environments described by the two V(V) models, **D** and **F**. Notably, the data from samples **A2a** and **D2b**, where the XAS fits suggested contributions from coordination environments that are mimicked by both models **D** and **F** (Figure 6b), were the ones that stood out in the PCA of the data (Figure 4a), but the reasons for this difference are not yet clear. Most of the best fits to the XAS for samples **A2**−**D2** (as well as those for **A3**−**D3** and **A4**−**D4**, Figure 6c,d) contained small but significant proportions (7−15% mol; Table S1) of XAS of an octahedral nonoxido V(IV) model, **H** (Chart 1).

The best XANES fits for V-treated isolated plasma and serum samples (**A3**−**D3** and **A4**−**D4** in Table 1 and Figure 6c,d) were distinguished from those from the blood plasma fractions (**A2**−**D2** in Figure 6b) mainly by the higher proportions of XANES from V(V) models, **D** and **F** (Chart 1). For the XANES data collected at AS, similar fits were obtained for the reaction products with either plasma or serum (Figure 6c,d), in agreement with close grouping of these data in PCA scores plots (green and blue dots in Figure 4a). However, these fits underestimated the proportion of V(V) in the samples, due to significant photoreduction during the data collection (Figures 5 and S2). Best fits to the XANES data collected at ANBF (designated as **A3b***, **C3b***, **A4b***, and **C4b*** in Figures 6c,d) suggested complete replacement of V(IV) with V(V) species compared with those from the corresponding samples of blood plasma fractions (**A2b*** and **C2b*** in Figure 6b), including the appearance of XANES from two new V(V) models, **A** and **I** (Chart 1). Similar best fits were obtained for the XANES from the decomposition products of **A**−**D** in plasma or serum at either 1 or 6 h of incubation time (e.g., **A3a** and **A3b** in Figure 6c), which indicated that these reactions were mostly complete within 1 h.

Vanadium Speciation in the Reaction Products with Isolated Blood Proteins. The reaction products of vanadate with bovine serum albumin or transferrin (1:1 V to protein molar ratio; samples **A**-BSA and **A**-Tf in Table 1) were highly susceptible to photoreduction at AS, as shown by comparison of XANES data for slow and rapid scans (2.0 and 0.50 s dwell time per point, respectively) in Figure 7a,b. Notably, the photoreduction product of **A**-Tf (black line in Figure 7b) contained mostly V(III) species, as shown by comparison with XANES of a model V(III) catecholato complex, **G** (Chart 1) in Figure 7c. The XANES of the photoreduction product of **A**-BSA was close to that of a six-coordinate V(IV) complex, **E** (Chart 1 and Figure 7c), while the nonreduced **A**-BSA was likely to contain a mixture of V(IV) and V(V) species (from the first rapid XANES scan, red line in Figure 7a). This XANES spectrum, which was minimally affected by photoreduction, also resembled the typical XANES data for the reaction products of **A** with isolated plasma or serum, as illustrated in Figure 7d (black and red lines), while the rapid scan XANES of **A**-Tf was significantly different (green line in Figure 7d). The XANES of the reaction product of bovine met-hemoglobin with excess vanadate (**A**-Hb in Table 1) suggested the predominance of four- and five-coordinate V(V) species (Figure 8; the data were collected at ANBF and thus minimally affected by photoreduction).[41] This XANES spectrum did not match the data for V bio-transformation products in RBC that consisted predominantly of V(IV) species (Figure 6a), as illustrated in Figure 8. On the whole, these results show that the XANES spectra of V(V)−protein adducts (collected for freeze-dried samples at 295 K) must be interpreted with caution, as they are likely to be subjected to photoreduction.

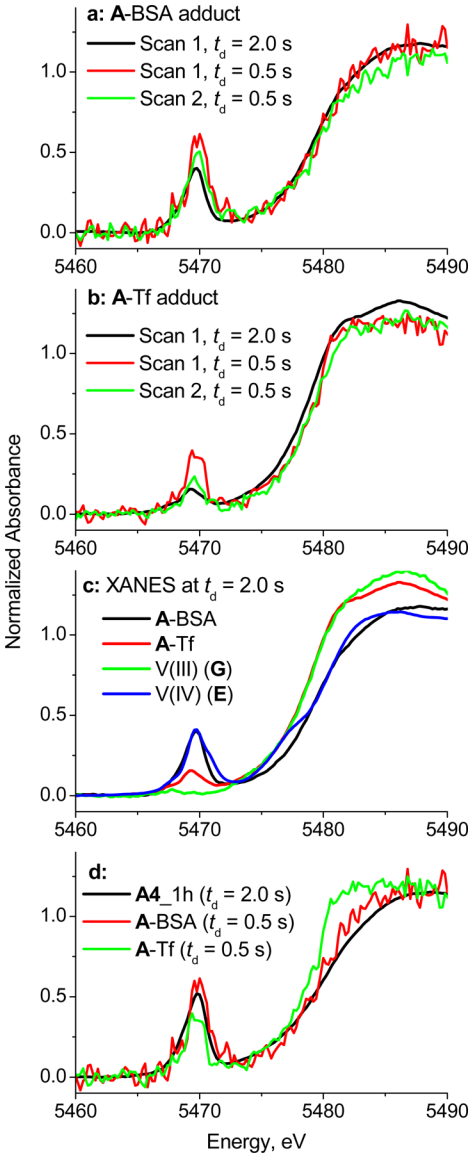

Figure 7. XANES data for V adducts with bovine serum albumin and apo-Tf (**A**-BSA and **A**-Tf in Table 1), collected at AS (freeze-dried samples, 295 K): (a) comparison of rapid and slow scans for **A**-BSA (t_d is dwell time per point); (b) comparison of rapid and slow scans for **A**-Tf; (c) comparison of XANES of **A**-BSA and **A**-Tf (slow scans) with those of model V(IV) and V(III) complexes (**E** and **G** in Chart 1); and (d) comparison of rapid XANES scans for **A**-BSA and **A**-Tf with the data for the reaction product of **A** with bovine serum (**A4**_1h in Table 1).

DISCUSSION

Reactivities of V(V/IV) Complexes in Isolated Plasma or Serum. Figure 2a,d illustrates the convergence of very different XANES from the initial compounds **A**−**D** (Chart 1) into nearly identical XANES of the reaction products with isolated rat plasma within 1 h at 310 K (conditions **A3**_1h to **D3**_1h in Table 1). Similar results were also obtained for the reactions with heat-inactivated bovine serum, as well as for longer reaction times (6 h at 310 K; **A3**_6h to **D3**_6h, **A4**_1h to **D4**_1h, and **A4**_6h to **D4**_6h in Table 1 and Figure 6).

DOI: 10.1021/acs.inorgchem.5b00665
Inorg. Chem. 2015, 54, 7753−7766

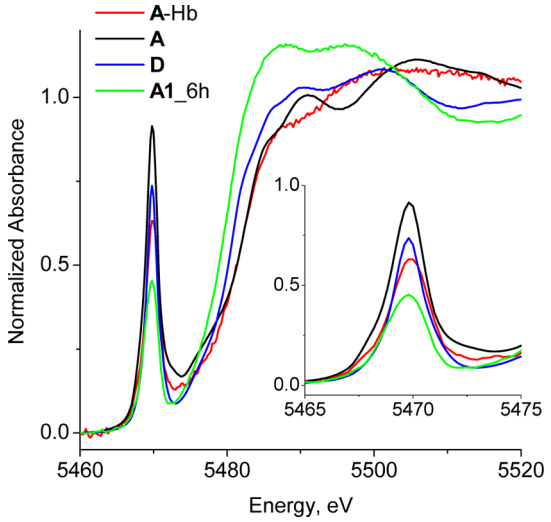

Figure 8. Comparison of XANES of a V adduct of bovine methemoglobin (**A**-Hb in Table 1, data collected at ANBF) with those of model V(V) complexes (**A** and **D** in Chart 1) and with typical XANES of the bio-transformation product of **A** in red blood cells (sample **A1**_6h in Table 1).

Multiple linear regression analyses of XANES data collected at the ANBF, where photoreduction was minimal,[41] provided strong evidence that these samples contained V(V) species only, which are represented by model complexes **A**, **D**, **F**, and **I** in Chart 1 (samples **A3***, **C3***, **A4***, and **C4*** in Figure 6c,d). These results are consistent with rapid (~1 h at 310 K) oxidation of V(IV) to V(V) by aerial oxygen in isolated serum, which was observed by EPR spectroscopy.[57] Significant photoreduction of these samples at the AS (Figures 5 and S2) resulted in the formation of V(IV) products (modeled as **B** and **G** in Figure 6c,d). The effects of photoreduction were even stronger in the reaction products of **A** with isolated serum proteins (albumin or transferrin, Figure 7). These results emphasized the need to consider the effects of photoreduction on speciation studies of metal compounds (particularly those in high oxidation states) in biological matrices.[41] However, since the most biologically relevant samples with respect to V speciation in blood were those from red blood cells (where there was no discernible photodamage) and in plasma fraction (where there is only a very small amount of photodamage, Figure 5 and Supporting Information, Figure S2), the photodamage observed in the isolated serum and blood samples do not affect the conclusions of the research.

The high proportions of XANES from models **D** and **F** in the best fits (Figure 6c,d) are likely to represent V(V) binding to typical donor groups of proteins and 2-hydroxyacid groups of certain carbohydrates, or of small biomolecules, such as citrate (modeled by a 2-hydroxycarboxylato complex, **F**).[25,30] The presence of XANES from model **A** in the best fit points to the likely formation of free mono- or oligonuclear vanadates(V),[30a] while the XANES contributions from an octahedral nonoxido V(V) complex (corresponding to model **I** in Chart 1) probably represents V(V) binding to tyrosine groups of proteins, including transferrin as described below.[12b,c] These changes are illustrated by process (1) in Scheme 1, using typical antidiabetic V(IV) or V(V) complexes (**C** or **D** in Chart 1)[31,32] as examples.

In contrast to the extensive data published on V(V) and V(IV) binding to isolated blood proteins and other model systems,[11−14] no detailed speciation studies of such complexes in isolated plasma or serum have been performed thus far, apart from some computer modeling studies.[58] Several studies of V distribution between high- and low-molecular mass serum fractions have been performed by chromatographic or electrophoretic techniques,[59−63] but these results are likely to be affected by V redistribution under the experimental conditions,[26,27,64] and the oxidation states of V products were not determined. As shown herein, XANES spectroscopy is the method of choice for the determination of V oxidation states and coordination environments in whole serum or plasma, as long as the issue of photodamage is addressed.[28,41] Studies are under way to obtain photodamage-free XANES data for V(V)- and V(IV)-protein adducts (including those for oxygen-sensitive blood proteins such as deoxyhemoglobin), using electrochemical X-ray absorption spectroscopy techniques.

Forms of Vanadium that Enter the Blood. Our previous studies[30] have shown that typical antidiabetic V(V) and V(IV) complexes, such as **C** and **D**,[31,32] undergo extensive transformations in gastrointestinal media (unless they are protected by anionic polysaccharides),[30b] which are illustrated by process (2) in Scheme 1. The main reaction products are V(IV) citrato or carbohydrato complexes with 2-hydroxyacidato ligands (both modeled by **B**) or vanadates(V) (modeled by **A**) in the presence or absence of typical food components, respectively, while V(III) is formed as a minor species in acidic medium of the stomach in the presence of reductants (such as ascorbate from food).[30a] The resulting products are likely to be absorbed by intestinal epithelial cells[65] and undergo further transformations, but no information on such processes is currently available.[30] It is, therefore, assumed that orally ingested V enters the blood plasma in a similar state to that formed in the gastrointestinal media (process (3) in Scheme 1). Nevertheless, direct absorption of **C**, **D** or their analogues from the digestive tract into the bloodstream is likely, to a limited extent, particularly in the absence of food (process (4) in Scheme 1).[2,30,66] Therefore, studies on the interactions of **C** and **D** with whole blood are also reported herein, along with those of the models of their decomposition products in gastrointestinal media (**A** and **B**).[30] Transformations of antidiabetic V complexes in gastrointestinal media have been overlooked in most of the previous studies, which have focused on the reactions of intact V(V) and V(IV) complexes (such as **C**, **D** or their analogues) with components of blood plasma,[11−14,67] or with isolated RBC.[21,22]

Uptake and Metabolism of Vanadium by Red Blood Cells. As shown in Figure 1 (black and green lines), compounds **A** and **C** are efficiently taken up by RBC within 1 h after the addition to whole blood at 310 K. These results are consistent with those in the literature,[15,17−21,63] which suggest that $[H_2VO_4]^-$ (the main form of **A** at low concentrations in neutral aqueous solutions)[10,68,69] is actively transported into RBC through phosphate channels,[15,17−19] while neutral lipophilic complexes like **C** can penetrate RBC membranes by passive diffusion.[14,20−22] The abrupt termination of further increases in RBC V content after 1 h of reaction with either **A** or **C** (Figure 1) was probably due to the conversion of these complexes into their reaction products with blood plasma proteins (Figure 2c), which did not enter RBC to any significant extent.[18] Complex **D** is capable of entering RBCs through passive diffusion at 273−277 K (zero time point in Figure 1a), but its low stability at pH = 7.4[32] meant that the original compound was likely to have decomposed immediately

DOI: 10.1021/acs.inorgchem.5b00665
Inorg. Chem. 2015, 54, 7753−7766

Scheme 1. Proposed Main Metabolic Pathways of Antidiabetic V(V) and V(IV) Complexes in Gastrointestinal Media and in the Blood[a]

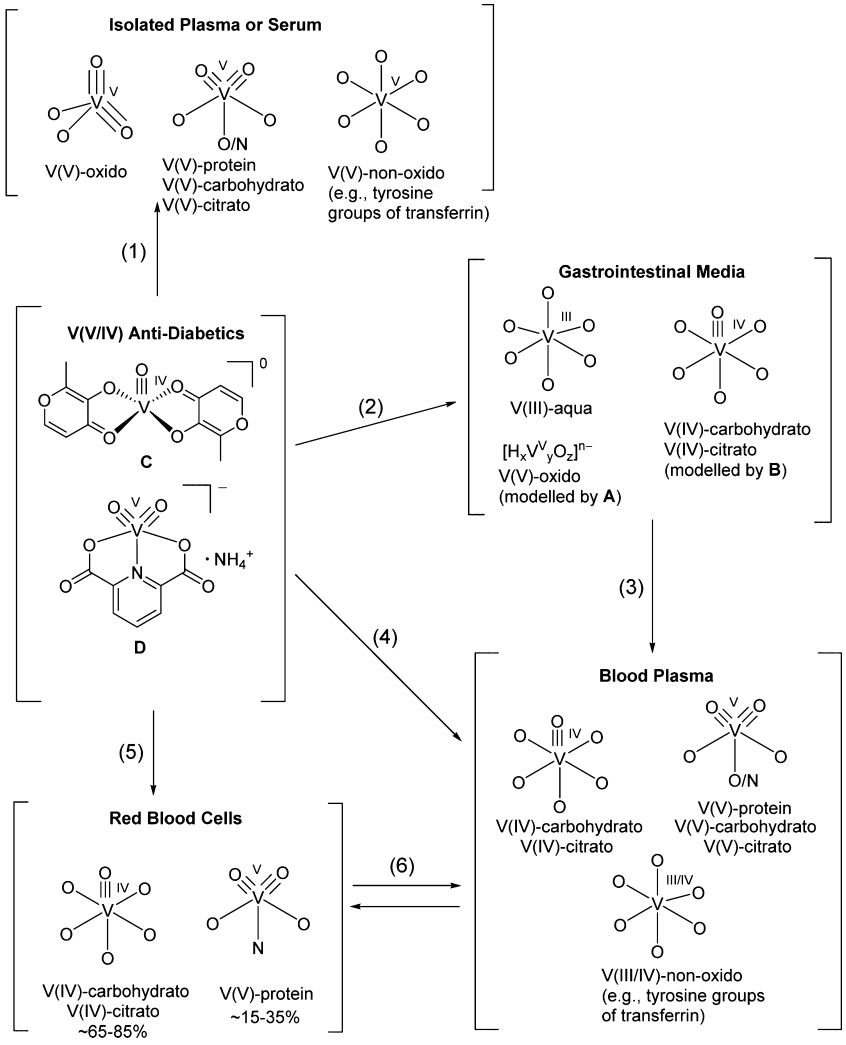

[a]On the basis of data of refs 12c and 30a and this work.

after the temperature was raised to 310 K, hence, its slower RBC uptake rates compared with those of either **A** or **C** (blue lines in Figure 1). Complex **B**, as a highly charged hydrophilic compound (Chart 1), was not expected to be permeable to RBC membranes to any significant extent,[64] as was confirmed by its low uptake values (red lines in Figure 1). These results suggested that if oral antidiabetics such as **C** were absorbed into the blood from gastrointestinal tract with the ligands still bound to V,[2,30] they would also enter RBC to some extent before being decomposed in the plasma (processes (4) and (5) in Scheme 1).

There is an ongoing controversy in the literature over the extent of V uptake by RBCs following treatments of humans or animals with V antidiabetics.[12a,22] Studies that have shown efficient accumulation of V compounds by RBCs in vitro were typically performed using RBC suspensions in aqueous buffers, rather than in blood plasma.[17−22] An ∼10-fold decrease in relative V content in RBCs due to V binding to blood plasma proteins has been reported in an earlier publication,[14] but this observation was mostly overlooked in subsequent studies.[12a,22] Three studies that used intravenous injections of ^{48}V-labeled inorganic V salts into animals reported that the V content in the RBC fractions (relative to that in total blood) was <5%,[70] 14%,[64] or up to 50%.[15] One of the problems of such studies was the use of V sources that are nonbiological and unstable in aerated neutral aqueous media, such as $^{48}V^{III}Cl_3$ or $^{48}V^{IV}OCl_2$,[70] although the use of $[^{48}V^{V}O_4]^{3-}$ in the latter two studies[15,64] was more biologically relevant. Despite the lack of reliable experimental data, it was generally assumed that the role of V uptake into RBCs was negligible compared with its binding to plasma proteins.[12a] Although the present results (Figure 1) and recently published data[22] (both using V concentrations of 0.50−1.0 mM) cannot be directly extrapolated to the low micromolar V concentrations that are expected to exist in the blood following oral administration of V antidiabetics,[12a,71] they support the view that RBCs are likely to play a significant role in the pharmacokinetics of these compounds.[15]

Remarkably reproducible XANES spectra of V-treated RBC fractions (Figures 2b, 4a, 6a, S2 and S3) were obtained using different initial V compounds (**A**−**D**), treatment times (1 or 6 h), beamlines (AS or ANBF, Figure S2), or V concentrations in the samples (V content in RBC after the reactions with **B** was ∼fivefold lower than that for the reactions with **A**, **C**, or **D**, Figure 1). These data implied the existence of an active

DOI: 10.1021/acs.inorgchem.5b00665
Inorg. Chem. 2015, 54, 7753−7766

metabolic pathway that converts various V complexes (e.g., either **A** or **C**) into the same final products, which are likely to consist mostly of V(IV)-carbohydrato or citrato complexes with 2-hydroxyacid donor groups (~65−85%; modeled by **B** and **E**) and V(V)−protein complexes (~15−35%; modeled by **D**), as shown in Figure 6a and Scheme 1. The latter species may correspond to V(V)−Hb complexes, such as **A**-Hb in Table 1 and Figure 8. The distinct V XANES spectra of RBC fractions, obtained in the research reported herein, can be used as a basis for attempts to characterize isolated V-containing species from RBCs, where XANES spectroscopy can be employed to monitor the identity and purity of the isolated products[29a] and, hence, to optimize conditions for isolation.

Previous studies by EPR spectroscopy suggested that the metabolism of V(IV) or V(V) complexes by RBCs leads to binding of the resultant V(IV) species to O-, N-, and possibly S-donor groups of proteins (predominantly Hb as the most abundant protein in RBC).[21,22] However, these results were likely to be affected by the following factors: (i) the choice of mostly five-coordinate V(IV) oxido complexes as models for the analysis of EPR spectra of biological samples;[21] and (ii) the use of RBC suspensions in aqueous buffers, rather than in blood plasma,[21,22] which is likely to affect the stability and uptake of V(V/IV) complexes.[18] Results of XANES spectroscopy reported herein have shown clearly the predominance of six-coordinate V(IV) oxido complexes in the reaction products with blood components (Figures 3 and 6), and EPR spectroscopic characteristics of such species are different from those of five-coordinate V(IV) complexes.[72] Size exclusion chromatography of lysates of V-treated RBCs suggested V binding both to Hb and to low-molecular-mass ligands (1−4 kDa),[63,64] but these results are likely to be affected by changes in V speciation during the lysis and separation procedures.[26,27,29a] As shown in the in vitro studies, binding of V(IV) complexes to isolated met-Hb is relatively weak and nonspecific,[22,73] although the formation of V(IV)−Hb adducts during the reduction of V(V) by deoxy-Hb is an option yet to be explored (for example, by the electrochemical XANES technique described above).

Speciation of Vanadium in the Plasma Fraction of Whole Blood. A crucial finding of this work was the significant difference in XANES of plasma fractions of whole blood compared with those of isolated plasma or serum samples (Figures 4a and 5b,d). Generally, V in blood plasma isolated from treated whole blood was in a more reduced state than when isolated plasma was treated; this difference was particularly striking when photoreduction of the samples was minimized[41] (ANBF data in Figures 5b,d and 6). These results are consistent with those of the RBC uptake studies (Figure 1), as well as with the literature data,[18] which suggested that V species can be exchanged between RBCs and plasma fractions of whole blood (process (6) in Scheme 1). They are also consistent with long lifetimes of V(IV) species in whole rat blood (either ex vivo or in circulation), which were observed by EPR spectroscopy,[16] in contrast with rapid oxidations of typical antidiabetic V(IV) complexes[21,30,37] or V(IV)−protein adducts[57] to their V(V) analogues in aerated neutral aqueous solutions.

The XANES of the V(V) species present in the plasma fractions were best modeled by the use of XANES from **D** and/or **F** (Chart 1 and Figure 6b), which are likely to represent V(V) binding to protein, carbohydrate, or citrato ligands. The XANES of the major V(IV) species was fitted with XANES from model **B**, which is a likely model for V(IV)−carbohydrato or citrato complexes (Chart 1 and Figure 6b), with 2-hydroxyacid donor groups, or V(V/IV) mixed-valence complexes with similar donors.[30,74] These data are consistent with the results of EPR spectroscopic and potentiometric studies that predict a significant role of V(V) and V(IV)−citrato species in blood plasma.[11−13] Although **B** was not efficiently taken up by RBCs (Figure 1), the role of citrato ligands in V transport into other cell types is likely to be more prominent, since active transport mechanisms for metal citrates are known to exist in such cells.[75]

Minor components of XANES from V(IV) species that were present in most of the plasma and serum samples (modeled with XANES from **H** in Chart 1 and Figure 7b−d) are likely to represent V(IV) binding to tyrosine residues in the active site of transferrin (Tf, the main Fe(III) carrier protein).[12,69] Typically, 30−40 μM Tf is present in blood plasma, and it is loaded with Fe(III) by ~30%, which means that up to 40−55 μM V can bind to the vacant binding sites (two per Tf protein).[12,69] These numbers agree well with the expected V concentrations in most of the plasma fractions in equilibrium with RBCs (~0.5 mM, Figure 1b) and with the average content of XANES from model **H** in the XANES fits (~10%, Figure 7b and Table S1). Since the relative V(V) content was significantly higher in isolated plasma or serum samples compared with plasma fractions of whole blood (samples **A3***, **C3***, **A4***, and **C4*** in Figure 6c,d, where the effect of photoreduction was minimal),[41] further oxidation of V(IV)−Tf could occur, resulting in the formation of V(V)−Tf. This process corresponds to the appearance of XANES from model **I** (the oxidized analogue of **H**, Chart 1) in the fits to the XANES from **A3***, **C3***, **A4***, and **C4*** (Figure 6c,d). These results are consistent with the literature data on the preferential V(V) and V(IV) binding to Tf in blood plasma.[11−13] Importantly, at physiologically relevant concentrations (5−50 μM),[2,12a] most of the V in the plasma is expected to be bound to Tf, most likely in the V(IV) oxidation state.[11−13] Furthermore, the reducing influence of RBCs may promote the formation of V(III)−Tf complexes in blood plasma (driven by the strong affinity of V(III) as like Fe(III), to the active sites of Tf).[12c] Notably, V(III)−Tf adducts were formed from the reaction products of V(V) with apoTf at pH = 7.40 in the presence of excess carbonate (**A**-Tf in Table 1) under X-ray irradiation conditions (Figure 7b,c), which supports suggestions in the literature[12c] that the formation of V(III)−Tf in mammalian blood is feasible. However, multiple linear regression analyses of XANES data from the in vitro reaction products with rat blood (Figure 6 and Table S1) did not support the presence of measurable amounts of V(III) (modeled as **G** in Chart 1) in these samples, probably because any V(III)−Tf species are reoxidized by excess V(V) formed under the reaction conditions (≥0.25 mM, Table 1 and Figure 6c).

CONCLUSIONS

Roles of Red Blood Cells in the Metabolism of Antidiabetic V(V/IV) Complexes. In summary, the results of XANES spectroscopic studies of V metabolism in whole blood have implicated the following two roles of RBC in this process (Scheme 1): (i) uptake of V compounds, either by active transport ($[H_2VO_4]^-$) or by passive diffusion (V(IV) or V(V) complexes with organic ligands), and their conversion into well-defined V(IV) and V(V) metabolites; and (ii) the presence of a more reducing environment for V than in isolated

DOI: 10.1021/acs.inorgchem.5b00665
Inorg. Chem. 2015, 54, 7753−7766

blood plasma. The former function has certain similarities with the recently discovered As(III) detoxification mechanism in the blood in the presence of Se(IV) compounds, which involves the formation of stable $[(GS)_2AsSe]^-$ adducts (where GS is S-bound deprotonated glutathione) in RBCs.[76] Glutathione is known to be involved (directly or indirectly) in V(V) reduction by RBCs,[19] although the resultant V(IV) is predominantly O-bound (Figure 6a). A potential application of this function is the use of RBCs as vehicles for targeted delivery of V compounds to specific sites, including immune system or malignant tumors (due to the excessive permeability of blood vessels in the tumors).[77] The latter function is likely to promote the formation of V(IV) and/or V(III)−Tf adducts in the plasma,[11−13] which in turn would facilitate V uptake by insulin-sensitive cells (e.g., skeletal muscle or adipose tissue), and enhance the antidiabetic activity of V compounds,[2,4] as well as uptake by cancer cells, which are rich in transferrin receptors.[78] The latter may contribute to the well-known anticancer effects of certain vanadium complexes.[3,5,6]

The Use of XANES in Speciation of the V Pro-Drugs in Biological Samples. While the importance of V speciation in controlling the activities of biological systems has been recognized for many years,[10,79] the results reported here, and in our other recent papers,[25,30] highlight the new insights that can be obtained from using XANES in speciation. In a related paper, we also report the implications of this blood speciation for the uptake and speciation of V in target cells.[30c]

Broader Implications for the Modes of Actions of Metal Pro-Drugs. Metal pro-drugs are widely used in medicine to treat a large number of diseases,[80] but the roles of RBCs in changing their speciation and transporting them to the site of the disease have generally not been taken into account when considering the efficacy, toxicity, and pharmacokinetics of such drugs. The results reported here show that the role of RBCs in the metabolism of metal-containing drugs in the blood is no less important than that of serum proteins, such as albumin, immunoglobulins, or transferrin.[11−14]

■ ASSOCIATED CONTENT

Ⓢ Supporting Information

Tables summarizing the details of multiple linear regression analyses of XANES data; figures showing detailed comparison of XANES spectra of the samples (Table 1) and overlays of experimental and fitted XANES spectra. The Supporting Information is available free of charge on the ACS Publications website at DOI: 10.1021/acs.inorgchem.5b00665.

■ AUTHOR INFORMATION

Corresponding Author

*E-mail: peter.lay@sydney.edu.au.

Notes

The authors declare no competing financial interest.

■ ACKNOWLEDGMENTS

The research was supported by Australian Research Council (ARC) Discovery Grants (DP0208409, DP0774173, DP0984722, DP1095310, and DP130103566), ARC Professorial Fellowships (DP0208409 and DP0984722) to P.A.L., and an ARC Linkage Infrastructure, Equipment and Facilities (LIEF) Program Grant (LE0346515) for the 36-pixel Ge detector at ANBF. X-ray absorption spectroscopy was undertaken at the X-ray absorption spectroscopy beamline at the Australian Synchrotron, Victoria, Australia, as well as at the Australian National Beamline Facility at the Photon Factory in Japan with support from the Australian Synchrotron Research Program (ASRP), which was funded by the Commonwealth of Australia under the Major National Research Facilities program (ANBF was operated by the Australian Synchrotron (AS) from 2009 until its closure in 2013). We acknowledge the LIEF program of the ARC for financial support (Grant Nos. LE0989759 and LE110100174) and the High Energy Accelerator Research Organisation (KEK) in Tsukuba, Japan, for operations support. We thank Dr. T. Bonin (Univ. of Sydney) for the help with blood sample collection, Drs. G. Foran, J. Hester, C. Fong, and M. Cheah for the assistance with XAS experiments at ANBF, and Drs. G. Devlin and P. Kappen for those at the AS.

■ ABBREVIATIONS

ANBF, Australian National Beamline Facility; AS, Australian Synchrotron; citr, citrato(4-); dipic, pyridine-2,6-dicarboxylato-(2-); Hb, hemoglobin; HBS, HEPES buffered saline; HEPES, 4-(2-hydroxyethyl)piperazine-1-ethanesulfonic acid; ma, maltolato(−); PC, principle component; PCA, principle component analysis; RBC, red blood cells; Tf, transferrin; XANES, X-ray absorption near-edge structure

■ REFERENCES

(1) Evangelou, A. M. *Crit. Rev. Oncol. Hematol.* **2002**, *42*, 249−265.
(2) Thompson, K. H.; Orvig, C. *J. Inorg. Biochem.* **2006**, *100*, 1925−1935.
(3) Barrio, D. A.; Etcheverry, S. B. *Curr. Med. Chem.* **2010**, *17*, 3632−3642.
(4) Levina, A.; Lay, P. A. *Dalton Trans.* **2011**, *40*, 11675−11686.
(5) (a) Benítez, J.; Becco, L.; Correia, I.; Leal, S. M.; Guiset, H.; Pessoa, J. C.; Lorenzo, J.; Tanco, S.; Escobar, P.; Moreno, V.; Garat, B.; Gambino, D. *J. Inorg. Biochem.* **2011**, *105*, 303−312. (b) Costa Pessoa, J.; Etcheverry, S.; Gambino, D. *Coord. Chem. Rev.* **2015**, in press, doi 10.1016/j.ccr.2014.12.002.
(6) (a) Rehder, D. *Future Med. Chem.* **2012**, *4*, 1823−1837. (b) Rehder, D. *Dalton Trans.* **2013**, *42*, 11749−11761.
(7) Wang, B.; Tanaka, K.; Morita, A.; Ninomiya, Y.; Maruyama, K.; Fujita, K.; Hosoi, Y.; Nenoi, M. *J. Radiat. Res.* **2013**, *54*, 620−629.
(8) Paglia, D. N.; Wey, A.; Hreha, J.; Park, A. G.; Cunningham, C.; Uko, L.; Benevenia, J.; O'Connor, J. P.; Lin, S. S. *J. Orthop. Res.* **2014**, *32*, 727−734.
(9) Missaoui, S.; Ben Rhouma, K.; Yacoubi, M.-T.; Sakly, M.; Tebourbi, O. *J. Diabetes Res.* **2014**, *2014*, 1−7.
(10) (a) Akabayov, S. R.; Akabayov, B. *Inorg. Chim. Acta* **2014**, *420*, 16−23. (b) McLauchlan, C. C.; Peters, B. J.; Willsky, G. R.; Crans, D. C. *Coord. Chem. Rev.* **2015**, in press, doi 10.1016/j.ccr.2014.12.012.
(11) Jakusch, T.; Dean, A.; Oncsik, T.; Benyei, A. C.; Di Marco, V.; Kiss, T. *Dalton Trans.* **2010**, *39*, 212−220.
(12) (a) Costa Pessoa, J.; Tomaz, I. *Curr. Med. Chem.* **2010**, *17*, 3701−3738. (b) Mehtab, S.; Gonçalves, G.; Roy, S.; Tomaz, A. I.; Santos-Silva, T.; Santos, M. F. A.; Romao, M. J.; Jakusch, T.; Kiss, T.; Pessoa, J. C. *J. Inorg. Biochem.* **2013**, *121*, 187−195. (c) Costa Pessoa, J.; Gonçalves, G.; Roy, S.; Correia, I.; Mehtab, S.; Santos, M. F. A.; Santos-Silva, T. *Inorg. Chim. Acta* **2014**, *420*, 60−68.
(13) (a) Sanna, D.; Micera, G.; Garribba, E. *Inorg. Chem.* **2010**, *49*, 174−187. (b) Sanna, D.; Micera, G.; Garribba, E. *Inorg. Chem.* **2011**, *50*, 3717−3728. (c) Sanna, D.; Biro, L.; Buglyo, P.; Micera, G.; Garribba, E. *J. Inorg. Biochem.* **2012**, *115*, 87−99. (d) Sanna, D.; Micera, G.; Garribba, E. *Inorg. Chem.* **2013**, *52*, 11975−11985.
(14) Makinen, M. W.; Salehitazangi, M. *Coord. Chem. Rev.* **2014**, *279*, 1−22.
(15) Harris, W. R.; Friedman, S. B.; Silberman, D. *J. Inorg. Biochem.* **1984**, *20*, 157−169.

DOI: 10.1021/acs.inorgchem.5b00665
Inorg. Chem. 2015, 54, 7753−7766

(16) (a) Yasui, H.; Takechi, K.; Sakurai, H. *J. Inorg. Biochem.* **2000**, *78*, 185−196. (b) Yasui, H.; Tamura, A.; Takino, T.; Sakurai, H. *J. Inorg. Biochem.* **2002**, *91*, 327−338. (c) Yasui, H.; Adachi, Y.; Katoh, A.; Sakurai, H. *JBIC, J. Biol. Inorg. Chem.* **2007**, *12*, 843−853.
(17) (a) Cantley, L. C.; Resh, M. D.; Guidotti, G. *Nature* **1978**, *272*, 552−554. (b) Cantley, L. C.; Aisen, P. *J. Biol. Chem.* **1979**, *254*, 1781−1784.
(18) Heinz, A.; Rubinson, K. A.; Grantham, J. J. *J. Lab. Clin. Med.* **1982**, *100*, 593−611.
(19) Garner, M.; Reglinski, J.; Smith, W. E.; McMurray, J.; Abdullah, I.; Wilson, R. *JBIC, J. Biol. Inorg. Chem.* **1997**, *2*, 235−241.
(20) Yang, X.; Wang, K.; Lu, J.; Crans, D. C. *Coord. Chem. Rev.* **2003**, *237*, 103−111.
(21) Delgado, T. C.; Tomaz, A. I.; Correia, I.; Costa Pessoa, J.; Jones, J. G.; Geraldes, C. F. G. C.; Castro, M. M. C. A. *J. Inorg. Biochem.* **2005**, *99*, 2328−2339.
(22) (a) Sanna, D.; Serra, M.; Micera, G.; Garribba, E. *Inorg. Chem.* **2014**, *53*, 1449−1464. (b) Sanna, D.; Serra, M.; Micera, G.; Garribba, E. *Inorg. Chim. Acta* **2014**, *420*, 75−84.
(23) Willsky, G. R.; Halvorsen, K.; Godzala III, M. E.; Chi, L.-H.; Most, M. J.; Kaszynski, P.; Crans, D. C.; Goldfine, A. B.; Kostyniak, P. J. *Metallomics* **2013**, *5*, 1491−1502.
(24) (a) Ueki, T.; Michibata, H. *Coord. Chem. Rev.* **2011**, *255*, 2249−2257. (b) Yamamoto, S.; Matsuo, K.; Michibata, H.; Ueki, T. *Inorg. Chim. Acta* **2014**, *420*, 47−52.
(25) Levina, A.; McLeod, A. I.; Lay, P. A. *Chem. - Eur. J.* **2014**, *20*, 12056−12060.
(26) De Cremer, K.; De Kimpe, J.; Cornelis, R. *Fresenius' J. Anal. Chem.* **1999**, *363*, 519−522.
(27) Nischwitz, V.; Davies, J. T.; Marshall, D.; González, M.; Gómez Ariza, J. L.; Goenaga-Infante, H. *Metallomics* **2013**, *5*, 1685−1697.
(28) (a) Aitken, J. B.; Levina, A.; Lay, P. A. *Curr. Top. Med. Chem.* **2011**, *11*, 553−571. (b) Hummer, A. A.; Rompel, A. *Metallomics* **2013**, *5*, 597−614.
(29) (a) Levina, A.; Harris, H. H.; Lay, P. A. *J. Am. Chem. Soc.* **2007**, *129*, 1065−1075. (b) Nguyen, A.; Mulyani, I.; Levina, A.; Lay, P. A. *Inorg. Chem.* **2008**, *47*, 4299−4309. (c) Levina, A.; McLeod, A. I.; Seuring, J.; Lay, P. A. *J. Inorg. Biochem.* **2007**, *101*, 1586−1593. (d) Levina, A.; Aitken, J. B.; Gwee, Y. Y.; Lim, Z. J.; Liu, M.; Singharay, A. M.; Wong, P. F.; Lay, P. A. *Chem. - Eur. J.* **2013**, *19*, 3609−3619. (e) Liu, M.; Lim, Z. J.; Gwee, Y. Y.; Levina, A.; Lay, P. A. *Angew. Chem., Int. Ed.* **2010**, *49*, 1661−1664.
(30) (a) Levina, A.; McLeod, A. I.; Kremer, L.; Aitken, J. B.; Glover, C. J.; Johannessen, B.; Lay, P. A. *Metallomics* **2014**, *6*, 1880−1888. (b) Kremer, L. E.; McLeod, A. I.; Aitken, J. B.; Levina, A.; Lay, P. A. *J. Inorg. Biochem.* **2015**, *147*, 227−234. (c) Levina, A.; McLeod, A. I.; Pulte, A.; Aitken, J. B.; Lay, P. A. *Inorg. Chem.* **2015**, *54*, 6707−6718.
(31) McNeill, J. H.; Yuen, V. G.; Hoveyda, H. R.; Orvig, C. *J. Med. Chem.* **1992**, *35*, 1489−1491.
(32) Crans, D. C.; Yang, L.; Jakusch, T.; Kiss, T. *Inorg. Chem.* **2000**, *39*, 4409−4416.
(33) Ballhausen, C. J.; Gray, H. B. *Inorg. Chem.* **1962**, *1*, 111−122.
(34) Winkler, J. R.; Gray, H. B. *Struct. Bonding (Berlin)* **2012**, *142*, 17−28.
(35) Tsaramyrsi, M.; Kaliva, M.; Salifoglou, A.; Raptopoulou, C. P.; Terzis, A.; Tangoulis, V.; Giapintzakis, J. *Inorg. Chem.* **2001**, *40*, 5772−5779.
(36) Nuber, B.; Weiss, J.; Wieghardt, K. *Z. Naturforsch., B: J. Chem. Sci.* **1978**, *33B*, 265−267.
(37) Orvig, C.; Gelmini, L.; Glover, N.; Herring, F. G.; Li, H.; McNeill, J. H.; Rettig, S. J.; Setyawati, I. A.; Shuter, E.; Sun, Y.; Tracey, A. S.; Yuen, V. G.; Caravan, P. *J. Am. Chem. Soc.* **1995**, *117*, 12759−12770.
(38) Wieghardt, K. *Inorg. Chem.* **1978**, *17*, 57−64.
(39) Glover, C.; McKinlay, J.; Clift, M.; Barg, B.; Boldeman, J.; Ridgway, M.; Foran, G.; Garret, R.; Lay, P.; Broadbent, A. *AIP Conf. Proc.* **2007**, *882*, 884−886.
(40) Thompson, A. C.; Attwood, D. T.; Gullikson, E. M.; Howells, M. R.; Kortright, J. B.; Robinson, A. L.; Underwood, J. H.; Kim, K.-J.; Kirz, J.; Lindau, I.; Pianetta, P.; Winick, H.; Williams, G. P.; Scofield, J. H. *X-ray Data Booklet,* 2nd ed.; University of California: Berkeley, CA, 2001.
(41) George, G. N.; Pickering, I. J.; Pushie, M. J.; Nienaber, K.; Hackett, M. J.; Ascone, I.; Hedman, B.; Hodgson, K. O.; Aitken, J. B.; Levina, A.; Glover, C.; Lay, P. A. *J. Synchrotron Radiat.* **2012**, *19*, 875−886.
(42) Milsmann, C.; Levina, A.; Harris, H. H.; Foran, G. J.; Turner, P.; Lay, P. A. *Inorg. Chem.* **2006**, *45*, 4743−4754.
(43) (a) Ellis, P. J.; Freeman, H. C. *J. Synchrotron Radiat.* **1995**, *2*, 190−195. (b) *XFit* for Windows, beta-version; Australian Synchrotron Research Program: Sydney, Australia, 2004.
(44) Weng, T.-C.; Waldo, G. S.; Penner-Hahn, J. E. *J. Synchrotron Radiat.* **2005**, *12*, 506−510.
(45) McMaster, W. H.; Kerr Del Grande, N.; Mallett, J. H.; Hubbell, J. H. *Compilation of X-ray Cross Sections;* Lawrence Livermore National Laboratory: Livermore, CA, 1969.
(46) *Unscrambler* Version 9.5, Camo Process AS: Oslo, Norway, 2005.
(47) *Microcal Origin,* Version 6.0; Microcal Software Inc.: Northampton, MA, 1999.
(48) Chen, W.-C. *Different types of blood cells and their roles in the human body*. http://web.mit.edu/scicom/www/blood.html (accessed on 17.04.14).
(49) Weidemann, C.; Rehder, D.; Kuetgens, U.; Hormes, J.; Vilter, H. *Chem. Phys.* **1989**, *136*, 405−412.
(50) Sarangi, R. *Coord. Chem. Rev.* **2013**, *257*, 459−472.
(51) Chaurand, P.; Rose, J.; Briois, V.; Salome, M.; Proux, O.; Nassif, V.; Olivi, L.; Susini, J.; Hazemann, J.-L.; Bottero, J.-Y. *J. Phys. Chem. B* **2007**, *111*, 5101−5110.
(52) Giuli, G.; Paris, E.; Mungall, J.; Romano, C.; Dingwell, D. *Am. Mineral.* **2004**, *89*, 1640−1646.
(53) Ressler, T.; Wong, J.; Roos, J.; Smith, I. L. *Environ. Sci. Technol.* **2000**, *34*, 950−958.
(54) Korbas, M.; O'Donoghue, J. L.; Watson, G. E.; Pickering, I. J.; Singh, S. P.; Myers, G. J.; Clarkson, T. W.; George, G. N. *ACS Chem. Neurosci.* **2010**, *1*, 810−818.
(55) Krakowiak, J.; Lundberg, D.; Persson, I. *Inorg. Chem.* **2012**, *51*, 9598−9609.
(56) Hambley, T. W.; Judd, R. J.; Lay, P. A. *Inorg. Chem.* **1992**, *31*, 343−345.
(57) Chasteen, N. D.; Grady, J. K.; Holloway, C. E. *Inorg. Chem.* **1986**, *25*, 2754−2760.
(58) (a) Gorzsás, A.; Andersson, I.; Pettersson, L. *Eur. J. Inorg. Chem.* **2006**, *2006*, 3559−3565. (b) Jakusch, T.; Dean, A.; Oncsik, T.; Bényei, A. C.; Di Marco, V.; Kiss, T. *Dalton Trans.* **2010**, *39*, 212−220.
(59) Lustig, S.; Lampaert, D.; De Cremer, K.; De Kimpe, J.; Cornelis, R.; Schramel, P. *J. Anal. At. Spectrom.* **1999**, *14*, 1357−1362.
(60) Chéry, C. C.; De Cremer, K.; Dumont, E.; Cornelis, R.; Moens, L. *Electrophoresis* **2002**, *23*, 3284−3288.
(61) Nagaoka, M. H.; Akiyama, H.; Maitani, T. *Analyst* **2004**, *129*, 51−54.
(62) Jakusch, T.; Hollender, D.; Enyedy, E. A.; Gonzalez, C. S.; Montes-Bayon, M.; Sanz-Medel, A.; Costa Pessoa, J.; Tomaz, I.; Kiss, T. *Dalton Trans.* **2009**, 2428−2437.
(63) Iglesias-González, T.; Sánchez-González, C.; Montes-Bayón, M.; Llopis-González, J.; Sanz-Medel, A. *Anal. Bioanal. Chem.* **2012**, *402*, 277−285.
(64) De Cremer, K.; Van Hulle, M.; Chéry, C.; Cornelis, R.; Strijckmans, K.; Dams, R.; Lameire, N.; Vanholder, R. *JBIC, J. Biol. Inorg. Chem.* **2002**, *7*, 884−890.
(65) Pantopoulos, K.; Porwal, S. K.; Tartakoff, A.; Devireddy, L. *Biochemistry* **2012**, *51*, 5705−5724.
(66) Crans, D. C.; Trujillo, A. M.; Pharazyn, P. S.; Cohen, M. D. *Coord. Chem. Rev.* **2011**, *255*, 2178−2192.
(67) Dias, D. M.; Rodrigues, J. P. G. L. M.; Domingues, N. S.; Bonvin, A. M. J. J.; Castro, M. M. C. A. *Eur. J. Inorg. Chem.* **2013**, *2013*, 4619−4627.

DOI: 10.1021/acs.inorgchem.5b00665
Inorg. Chem. 2015, 54, 7753−7766

(68) Crans, D. C.; Smee, J. J.; Gaidamauskas, E.; Yang, L. *Chem. Rev.* **2004**, *104*, 849−902.
(69) Rehder, D. *Bioinorganic Vanadium Chemistry;* John Wiley & Sons: Chichester, U.K., 2008.
(70) Sabbioni, E.; Marafante, E.; Amantini, L.; Ubertalli, L.; Birattari, C. *Bioinorg. Chem.* **1978**, *8*, 503−515.
(71) Thompson, K. H.; Lichter, J.; LeBel, C.; Scaife, M. C.; McNeill, J. H.; Orvig, C. *J. Inorg. Biochem.* **2009**, *103*, 554−558.
(72) (a) Farrell, R. P.; Lay, P. A. *Appl. Magn. Reson.* **1996**, *11*, 509−519. (b) Barr-David, G.; Charara, M.; Codd, R.; Farrell, R. P.; Irwin, J. A.; Lay, P. A.; Bramley, R.; Brumby, S.; Ji, J.-Y.; Hanson, G. R. *J. Chem. Soc., Faraday Trans.* **1995**, *91*, 1207−1216.
(73) Macara, I. G.; Kustin, K.; Cantley, L. C., Jr. *Biochim. Biophys. Acta, Gen. Subj.* **1980**, *629*, 95−106.
(74) (a) Barr-David, G.; Hambley, T. W.; Irwin, J. A.; Judd, R. J.; Lay, P. A.; Martin, B. D.; Bramley, R.; Dixon, N. E.; Hendry, P. *Inorg. Chem.* **1992**, *31*, 4906−4908. (b) Codd, R.; Hambley, T. W.; Lay, P. A. *Inorg. Chem.* **1995**, *34*, 877−882.
(75) (a) Yokel, R. A.; Wilson, M.; Harris, W. R.; Halestrap, A. P. *Brain Res.* **2002**, *930*, 101−110. (b) Arezes, J.; Costa, M.; Vieira, I.; Dias, V.; Kong, X. L.; Fernandes, R.; Vos, M.; Carlsson, A.; Rikers, Y.; Porto, G.; Rangel, M.; Hider, R. C.; Pinto, J. P. *PLoS One* **2013**, *8*, e79870.
(76) Manley, S. A.; George, G. N.; Pickering, I. J.; Glass, R. S.; Prenner, E. J.; Yamdagni, R.; Wu, Q.; Gailer, J. *Chem. Res. Toxicol.* **2006**, *19*, 601−607.
(77) Muzykantov, V. R. *Expert Opin. Drug Delivery* **2010**, *7*, 403−427.
(78) Daniels, T. R.; Bernabeu, E.; Rodríguez, J. A.; Patel, S.; Kozman, M.; Chiappetta, D. A.; Holler, E.; Ljubimova, J. Y.; Helguera, G.; Penichet, M. L. *Biochim. Biophys. Acta, Gen. Subj.* **2012**, *1820*, 291−317.
(79) (a) Kiss, T.; Odani, A. *Bull. Chem. Soc. Jpn.* **2007**, *80*, 1691−1702. (b) Crans, D. C.; Woll, K. A.; Prusinskas, K.; Johnson, M. D.; Norkus, E. *Inorg. Chem.* **2013**, *52*, 12262−12275.
(80) (a) Hambley, T. W. *Dalton Trans.* **2007**, 4929−4937. (b) Hambley, T. W. *Science* **2007**, *318*, 1392−1393. (c) Mjos, K. D.; Orvig, C. *Chem. Rev.* **2014**, *114*, 4540−4563.

DOI: 10.1021/acs.inorgchem.5b00665
Inorg. Chem. 2015, 54, 7753−7766